

Space Charge Behavior in Oil-Impregnated Insulation Paper Reinforced with Nano-TiO₂

Rui-Jin Liao,^a Cheng Lv,^{a,*} Li-Jun Yang,^a Yi-Yi Zhang,^{a,b,*} and Tuan Liu^a

Oil-impregnated insulation paper is widely used in power transformers, and the insulation properties of oil-impregnated insulation paper play an important role in the reliability of power equipment. The formation and dynamics of space charge can affect the performance of insulation material. However, methods to improve the space charge distribution in oil-impregnated insulation paper are rarely reported. In this paper, space charge behavior in oil-impregnated insulation paper has been investigated using the pulsed electro-acoustic (PEA) technique. A series of measurements was applied when the oil-impregnated insulation paper reinforced with different nano-TiO₂ contents was subjected to various electric field strengths. The accumulation and decay of space charge are discussed, and the internal electric field strength distribution of oil-impregnated insulation paper is analyzed. The test results show that the space charge distribution is improved and the distortion rate of the internal electric field strength is reduced by adding nano-TiO₂ to the oil-impregnated insulation paper. The results show that the proposed method offers a new way to improve the properties of oil-impregnated insulation paper.

Keywords: Space charge; Oil-impregnated insulation paper; Pulsed electro-acoustic (PEA); Nano-TiO₂; Distortion rate

Contact information: a: State Key Laboratory of Power Transmission Equipment & System Security and New Technology, Chongqing University, Chongqing, 400044, China; b: FREEDM Systems Center, Department of Electrical and Computer Engineering, North Carolina State University, Raleigh, North Carolina, 27606, USA;

**Corresponding authors:* yiyizhang.cqu@gmail.com and lvcheng20050602135@163.com

INTRODUCTION

The converter transformer is the most important component in a HVDC system. The reliability and security of the converter transformer is very important. Oil-impregnated insulation paper has been used in converter transformers because of its low cost and desirable physical and electrical properties. With the development of the system voltage level, transformer insulation must be developed almost concurrently. Therefore, research that improves the insulation performance of oil-impregnated insulation paper has important practical significance.

The accumulation of space charge within oil-impregnated insulation paper is closely related to the insulation property of oil-impregnated insulation paper. The internal electric field strength can be distorted because of the accumulation of space charge. The localized electrical field strength may be strengthened or weakened (Boggs 2004; Hanley *et al.* 2003). Partial discharge or breakdown may occur in those places where the electrical field strength is strengthened; this can lead to premature failure of the insulation material (Zhang *et al.* 1996; Liu *et al.* 1989). To date, research has focused on the space

charge dynamics of oil-impregnated insulation paper affected by voltage level, temperature, and moisture (Morshuis and Jeroense 1997; Ciobanu *et al.* 2002; Tang *et al.* 2010; Zhou *et al.* 2009; Liu *et al.* 1998). Although studies have found that many nanoparticles improve the space charge distribution in insulation materials such as polyethylene and polyimide, there are no reports on how to improve the space charge distribution in oil-impregnated insulation paper (Fleming *et al.* 2005; Huang *et al.* 2009; Wang *et al.* 2009; Zha *et al.* 2010; Thelakkadan *et al.* 2011; Abd El-kader *et al.* 2009; Ahmad *et al.* 1992).

When TiO₂ particles are used in papermaking, it is well known that the TiO₂ particle can be attached to the cellulose surface. After the oil immersion process of insulation paper, the cellulose and TiO₂ are wrapped by oil. The unsaturated coordination state of the TiO₂ surface can capture electrons in the oil (Du *et al.* 2012), the effect may greatly change the space charge behavior in oil-impregnated insulation paper. Therefore nano-TiO₂ was chosen to reinforce oil-impregnated insulation paper in this paper.

The pulsed electroacoustic (PEA) technique was first developed in the 1980s. PEA has been widely used in space charge research because of its low cost and ease of implementation. The PEA method can allow space charges to be observed during poling, *i.e.*, under an electric field, and after electric field removal, *i.e.*, during depolarization, thus providing thorough information on space charge dynamics (Mazzanti *et al.* 2003). This method comprises a way to understand the physical processes taking place inside the dielectric materials and makes it possible to select materials and interfaces that minimize the risks of breakdown in HV applications. In this paper, the PEA technique was used to measure the space charge distribution. A series of measurements was carried out when the oil-impregnated insulation paper reinforced with different nano-TiO₂ contents was subjected to two different applied DC electric fields. The accumulation and the decay of space charge are discussed, and the internal electric field strength distribution in the oil-impregnated insulation paper reinforced with different nano-TiO₂ contents is analyzed.

EXPERIMENTAL

Raw Materials

The pulp board (softwood pulp, Taizhou Xinyuan Electrical Equipment, Taizhou, China) used for making insulation paper was beaten to about 400 mL Canadian standard freeness (CSF) in a valley beater.

Nano-TiO₂ (95ZX063, Shanghai MaiKun chemical company, ShangHai, China, with average particle diameter $d < 60$ nm, relative dielectric constant $\epsilon_r = 100 \epsilon_0$, conductivity $\sigma = 1 \times 10^{11}$ S/m) was used for reinforcing insulation paper. Anhydrous ethanol (analytical pure, ShuangShuang Chemical, ShanDong, China) was used as a solvent in the process of surface modification of nano-TiO₂.

Sodium hydroxide (analytical pure, Huludao City Chemical Reagent, Liaoning, China) was used to adjust the PH value in the process of surface modification of the nano-TiO₂. Silane coupling agent (Z-6030, Dow Corning Corporation, Michigan, USA) was used to modify the surface of the nano-TiO₂.

The oil for immersing insulation paper was conventional transformer mineral oil (25#, Sichuan chuanrun, ChengDu, China).

Surface modification of nano-TiO₂

Surface modification was carried out before the nano-TiO₂ was used for the reinforcement of the insulation paper. The process of the surface modification was as follows:

- (1) 50 g of nano-TiO₂ was weighed and placed in a 100 °C oven for 30 min.
- (2) 0.5 g of silane coupling agent was weighed and put into a beaker.
- (3) 100 mL of anhydrous ethanol was measured, and the pH value of the mixed solution was adjusted with sodium hydroxide.
- (4) Nano-TiO₂ was added into the mixed solution; then, the mixed solution was put into a three-necked flask and 400 mL of anhydrous ethanol was added.
- (5) The solution in the three-necked flask was heated by the water bath method while stirring constantly.
- (6) After finishing the reaction, the product was placed in a beaker and put into a 100 °C oven to dry for 24 h.

Preparation and Oil immersion Process of Insulation Paper

Firstly, the nano-TiO₂ that was modified by the silane coupling agent was dissolved in absolute ethanol (1:100 wt%) and the slurry was homogenized by vigorous agitation with a magnetic stir bar for 10 min. Secondly, the pulp was diluted to 0.4 wt% in deionized water and various wt% nano-TiO₂ were added. The mixtures were stirred for 5 min at 5000 rpm in a fiber disintegration device and were used to prepare the insulation paper. Thirdly, each wet insulation paper was dried at 105 °C for 5 min under vacuum. Insulation paper with a target basis weight of 120 g/m² was produced. Lastly, some insulation paper was immersed in oil, using the following steps:

- (1) Insulation paper was cut in circular samples with diameters of 4 cm and put into different glass bottles according to the type of paper.
- (2) All samples were put into the vacuum chamber and were dried at 90 °C for 48 h. After that, the temperature of the vacuum chamber was adjusted to 40 °C.
- (3) The mineral oil at 40 °C was infused into the glass bottles in the vacuum chamber to immerse samples for 24 h.

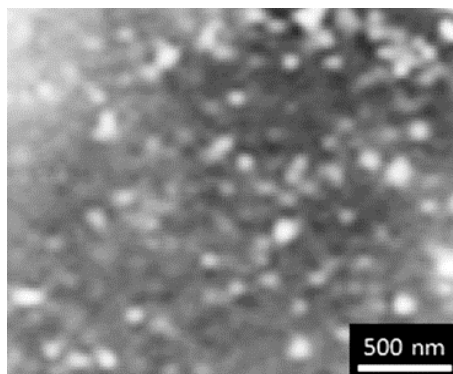


Fig. 1. SEM images of insulation paper reinforced with nano-TiO₂ after oil immersion process.

Experiment Characterization

The samples were stressed at two different DC electric field strengths (10 kV/mm and 30 kV/mm). Each time, an electrical stress time of 30 min was tested. In addition, when the applied DC electric field strength was 30 kV/mm, the space charge evolution after the removal of the applied electric field was measured at the same time.

Figure 1 shows the measurement equipment used in the PEA method. Acoustic pressure waves are generated due to the interaction of pulsed electric field and charge layer. Detection of acoustic pressure waves allows one to determine charge distribution across the sample.

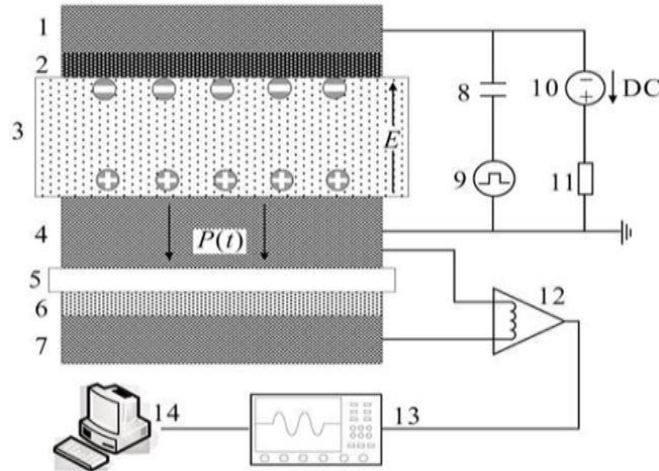


Fig. 2. Measurement equipment used in the PEA method

The principle of the pulsed-electro acoustic system (PEA) is described in many studies (Fothergill *et al.* 2000; Liu *et al.* 1993). The PEA system (PEANUT, made by Five Lab) used in this study has a pulse width of 5 ns. The bottom electrode is made of 10-mm-thick aluminum plate, and the top electrode is a semiconducting polymer to achieve a better acoustic match. The piezoelectric sensor used a 9- μm -thick LiNbO_3 material that enables the system to be heated up to 90 °C, although this was not utilized in the present study.

RESULTS AND DISCUSSION

Results

The nano- TiO_2 contents of the insulation paper were 0, 1%, and 3%, which were designated as P0, P1, and P3, respectively.

The space charge behavior in oil-impregnated insulation paper is different under different DC electric fields. Fig. 3 shows the space charge distribution of oil-impregnated insulation paper reinforced with different nano- TiO_2 contents in 30 min under a 10-kV/mm DC electric field.

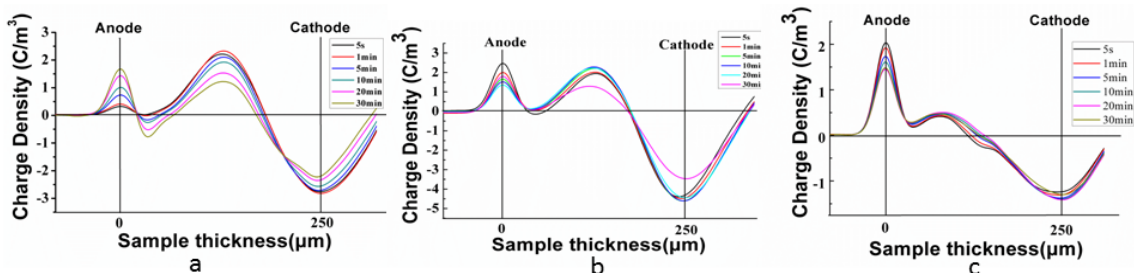


Fig. 3. The space charge distribution of oil-impregnated insulation paper reinforced with different nano- TiO_2 contents in 30 min under a 10-kV/mm DC electric field, a: P0, b: P1, c: P3

As shown in Fig. 3, the space charge injection phenomenon was observed at the electrodes. The peak value at the electrodes decreased with increasing nano-TiO₂ content. The space charge density on the anode decreased as the stressing time increased, while the space charge density on the cathode did not show regularity. The injection depth of negative charge from the cathode increased with increasing nano-TiO₂ content. As shown in Fig. 3a, the accumulation of negative space charge could be observed near the anode, but the negative space charges gradually disappeared as the time increased. After 5 min, the negative space charges could not be observed. In the middle of P0, the positive space charges were observed, and the positive space charge density increased as the time increased. In Fig. 3b, the accumulation of negative space charge was not observed near the anode. However, the positive space charges were observed in the middle of P1, and the positive space charge density in P1 increased as the time increased. As shown in Fig. 3c, the same as P1, the accumulation of negative space charge was not observed near the anode in P3, but there was an accumulation of a small amount of negative charges in the middle of P3. As time increased, the negative space charges gradually disappeared. The positive space charge density in P3 was much less than that in P0 and P1. The maximum space charge densities of P0, P1, and P3 were 3.61 C/m³, 2.53 C/m³, and 0.54 C/m³, respectively.

The electric field distribution in the sample due to the space charge can be calculated by integrating the charge density (Chen *et al.* 2004). The results of the electric field distribution in the sample can be directly obtained from the PEA. Figure 4 shows the internal electric field distribution of oil-impregnated insulation paper reinforced with different nano-TiO₂ contents in 30 min under a 10-kV/mm DC electric field.

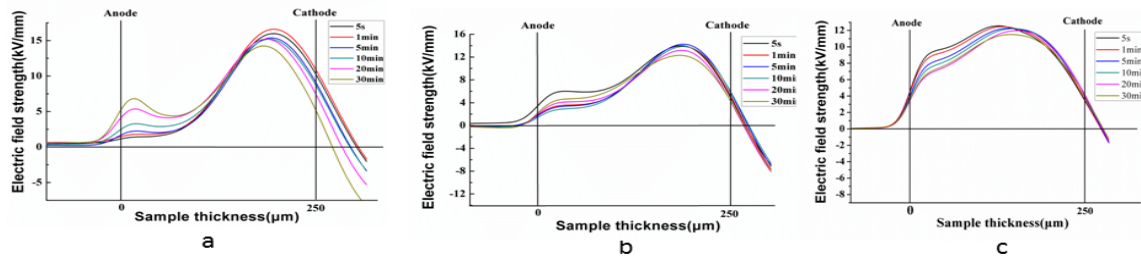


Fig. 4. The internal electric field distribution of oil-impregnated insulation paper reinforced with different nano-TiO₂ contents in 30 min under a 10-kV/mm DC electric field, a: P0, b: P1, c: P3

As shown in Fig. 4a, 4b, and 4c, the electric field strength was distorted: the electric field strength near the anode was weakened, and the electric field strength near the cathode was enhanced. The electric field strength became uniform as the stressing time increased. The maximum electric field strength in P0 declined as the stressing time increased, and the position of the maximum electric field strength moved away from the cathode gradually (Fig. 4a).

The position of maximum electric field strength in P1 did not change as the stressing time increased (Fig. 4b), but as shown in Fig. 4c, the position of maximum electric field strength in P3 remained close to the cathode. When the 10-kV/mm DC electric field was applied for 30 min, the maximum electric field distortions of P0, P1, and P3 were 67%, 45%, and 27%, respectively.

As shown in Fig. 5, the space charge density at the anode decreased as the stressing time increased, and the injection depth of positive charges of P0, P1, and P3 were the same. However, the injection depth of negative charges of P0, P1, and P3 were different; the injection of negative charge in P3 was the deepest, and the injection of negative charge in P0 was the shallowest.

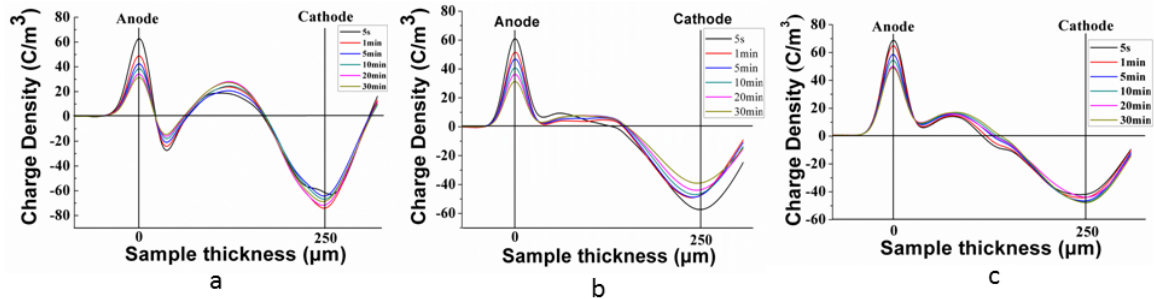


Fig. 5. The space charge distribution of oil-impregnated insulation paper reinforced with different nano-TiO₂ contents in 30 min under a 30-kV/mm DC electric field, a: P0, b: P1, c: P3

As shown in Fig. 5a, the accumulation of negative space charge could be clearly observed near the anode, and the negative space charges decreased as the stressing time increased. In the middle of P0, positive space charges increased as the time increased. In Fig. 5b, the positive space charges were observed everywhere, except for some negative charges observed near the cathode, and the positive space charges evenly distributed in P1. The variation of space charge of P3 was similar to the variation when the 10-kV/mm DC electric field was applied, and only the positive space charges exist in the area closer to the anode. The accumulation of negative space charge was observed in the middle of the P3, and as the time increased, the negative space charges gradually disappeared.

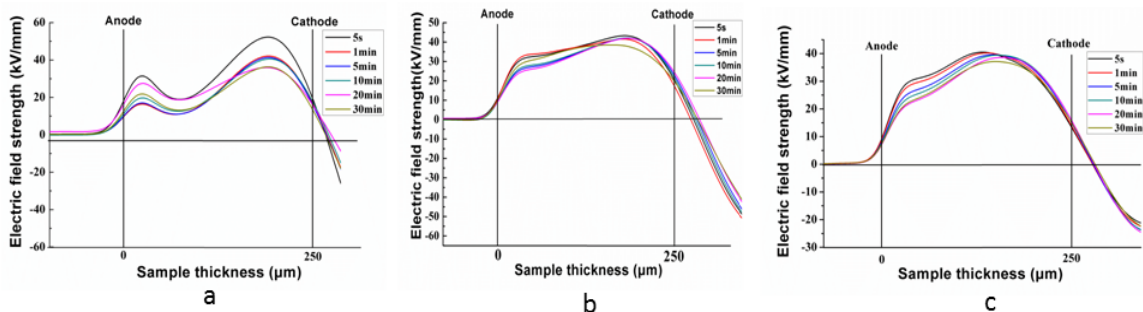


Fig. 6. The internal electric field distribution of oil-impregnated insulation paper reinforced with different nano-TiO₂ contents in 30 min under a 30-kV/mm DC electric field, a: P0, b: P1, c: P3

As shown in Fig. 6, the electric field strength also exhibited different levels of distortion. The electric field strength became uniform as the stressing time increased. As shown in Fig. 6a and 6b, in P0 and P1, the position of the maximum electric field strength is located near the anode and remained unchanged as the stressing time increased. In Fig. 6c, the position of maximum electric field strength in P3 changed and remained close to the cathode. When the 30-kV/mm DC electric field was applied for 30 min, the maximum electric field distortions of P0, P1, and P3 were 69%, 43%, and 33%, respectively.

Figure 7 shows the space charge decay of oil-impregnated insulation paper reinforced with different contents of nano-TiO₂ in 30 min after the removal of the 30-kV/mm DC field. As shown in Fig. 7, when the 30-kV/mm DC field was removed, negative space charges were induced in the anode. The space charges rapidly dissipated as the time increased. After 5 min, the space charge could still be observed in the interior of P0, but the space charge almost completely disappeared in the interior of P1 and P3. However, the space charge dissipation rates of P1 and P3 were slower than that of P0 at the electrodes.

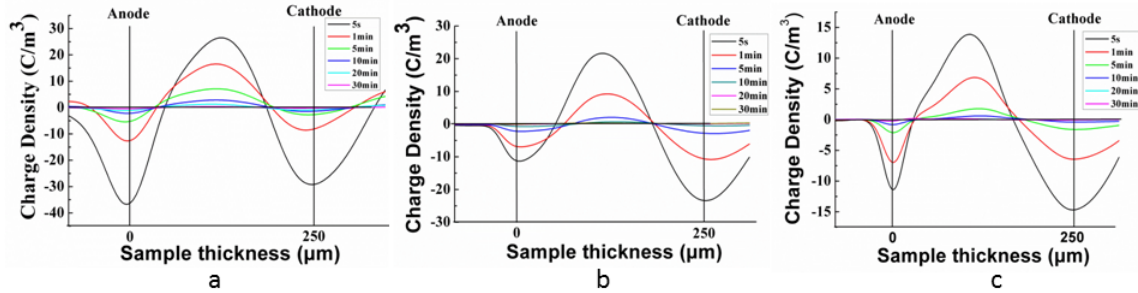


Fig. 7. Space charge decay of oil-impregnated insulation paper reinforced with different nano-TiO₂ contents in 30 min after the removal of the 30-kV/mm DC electric field, a: P0, b: P1, c: P3

The space charge amount of oil-impregnated insulation paper can be calculated using Equation 1,

$$Q(t) = \int_0^d |\rho(x, t)| S dx \quad (1)$$

where $\rho(x, t)$ is the internal charge density of oil-impregnated insulation paper, S is the surface area of the electrode, and d is the thickness of oil-impregnated insulation paper.

As shown in Table 1, the space charge amount of P0 increased as the time increased. The space charge amount of P1 increased firstly and then decreased with the time increase. There was little change in the space charge amount of P3 as the time increased.

Table 1. Space Charge Amount of Oil-Impregnated Insulation Paper Reinforced with Different Nano-TiO₂ Contents in 30 min under a 10-kV/mm DC Electric Field

Time	5 s	1 min	5 min	10 min	20 min	30 min
P0 (C)	3.69×10^{-7}	4.18×10^{-7}	4.63×10^{-7}	4.99×10^{-7}	5.39×10^{-7}	5.31×10^{-7}
P1 (C)	4.25×10^{-7}	4.55×10^{-7}	4.75×10^{-7}	4.92×10^{-7}	4.81×10^{-7}	3.73×10^{-7}
P3 (C)	1.88×10^{-7}	1.95×10^{-7}	1.93×10^{-7}	1.96×10^{-7}	1.98×10^{-7}	1.98×10^{-7}

A 10-kV/mm DC electric field was applied to the samples for 30 min, and the space charge amounts of P0, P1, and P3 were 5.31×10^{-7} C, 3.73×10^{-7} C, and 1.98×10^{-7} C, respectively. The space charge amount of the oil-impregnated insulation paper decreased with increasing nano-TiO₂ content. This shows that the addition of nano-TiO₂ can inhibit the injection of the space charges, and the effect of inhibition increases with increasing

nano-TiO₂ content. This result is consistent with other studies that showed that nanoparticles are used to improve organic polymers (Tian *et al.* 2011; Tomer *et al.* 2008).

Table 2. Space Charge Amount of Oil-Impregnated Insulation Paper Reinforced with Different Nano-TiO₂ Contents in 30 min under a 30-kV/mm DC Electric Field

Time	5 s	1 min	5 min	10 min	20 min	30 min
P0 (C)	6.22×10^{-6}	6.07×10^{-6}	5.65×10^{-6}	5.33×10^{-6}	5.33×10^{-6}	5.45×10^{-6}
P1 (C)	6.74×10^{-6}	6.22×10^{-6}	6.33×10^{-6}	6.33×10^{-6}	6.15×10^{-6}	6.13×10^{-6}
P3 (C)	6.46×10^{-6}	6.67×10^{-6}	6.71×10^{-6}	6.79×10^{-6}	6.79×10^{-6}	6.81×10^{-6}

As shown in Table 2, the space charge amount of P0 and P1 decreased as the time increased. However, the space charge amount of P3 increased as the stressing time increased. The 30-kV/mm DC electric field was applied to the samples for 30 min, and the space charge amount of oil-impregnated insulation paper achieved basic stability. The space charge amounts of P0, P1, and P3 were 5.45×10^{-6} C, 6.13×10^{-6} C, and 6.81×10^{-6} C, respectively. When the applied DC electric field was 30-kV/mm, the space charge amount of oil-impregnated insulation paper reinforced with nano-TiO₂ increased. The variation trend of the space charge is the opposite of the variation of space charge when the 10-kV/mm DC electric field was applied.

Table 3. Space Charge Amount of Oil-Impregnated Insulation Paper Reinforced with Different Nano-TiO₂ Contents in 30 min after Removal of the 30-kV/mm DC Electric Field

Time	5 s	1 min	5 min	10 min	20 min	30 min
P0 (C)	4.84×10^{-6}	2.59×10^{-6}	1.14×10^{-6}	4.5×10^{-7}	2.8×10^{-7}	1.25×10^{-7}
P1 (C)	3.91×10^{-6}	1.96×10^{-6}	6.25×10^{-7}	1.75×10^{-7}	-----	-----
P3 (C)	2.63×10^{-6}	1.22×10^{-6}	3.18×10^{-7}	0.94×10^{-7}	-----	-----

As shown in Table 3, after the removal of the 30-kV/mm DC electric field, the space charge amounts of P0, P1, and P3 decreased with increasing time. The speed of the space charge decays of P1 and P3 were faster than that of P0. Twenty minutes after the removal of the 30-kV/mm DC electric field, the space charge amounts of P1 and P3 were smaller than the measurement precision of the instrument.

Discussion

The space charges in the oil-impregnated insulation paper can be divided into two types according to detrapping rate. One is fast charges; the other one is slow charges. The fast charges are captured by shallow traps; the slow charges are captured by deep traps. When the applied DC electric field is removed, the fast charges can quickly detrapp and dissipate, and the detrapping speed and the dissipation speed of slow charges are slower than that of fast charges. When the DC electric field is applied, the space charge that is detected by PEA contains fast charges and slow charges. When the DC electric field is removed, the fast charges quickly detrapp and dissipate, and the space charges that are detected by PEA only contain slow charges. Therefore, the amount of fast charges is obtained using the space charge amount of the oil-impregnated insulation paper with the DC field minus the space charge amount of the oil-impregnated insulation paper without

the DC electric field. Because fast charges are captured by shallow traps, the amount of fast charges shows the amount of shallow traps. Tables 2 and 3 show that the amount of dissipation charge can be calculated. Five seconds after the removal of the electric field, the amounts of fast charges of P0, P1, and P3 were 0.61×10^{-6} C, 2.22×10^{-6} C, and 4.18×10^{-6} C, respectively.

After the 30-kV/mm DC electric field was applied for 30 min, the space charge amounts in P1 and P3 were more than that of P0. This shows an increase of P1 and P3 in the traps, but 5 s after the removal of the 30-kV/mm DC electric field, the space charge amounts of P1 and P3 were less than that of P0. This shows that these additional traps were shallow traps and that some deep traps were transformed into shallow traps because of the addition of nano-TiO₂. When the 30-kV/mm DC electric field was applied for 30 min, the negative space charge amount, which existed in the oil-impregnated insulation paper near the cathode, increased with increasing nano-TiO₂ content. Furthermore, the positive space charge amount, which existed in the middle of the oil-impregnated insulation paper decreased with increasing nano-TiO₂ content. These changes in space charge distribution can reinforce the electric field strength near the anode and weaken the electric field strength near the cathode; therefore, the internal electric field distribution becomes uniform.

CONCLUSIONS

1. When the applied electric field was 10-kV/mm DC, the space charge amount in the oil-impregnated insulation paper decreased with increasing nano-TiO₂ content. The maximum electric field distortions of P0, P1, and P3 were 67%, 45%, and 27%, respectively.
2. When the applied electric field was 30-kV/mm DC, the space charge amount in the oil-impregnated insulation paper increased with increasing nano-TiO₂ content. The maximum electric field distortions of P0, P1, and P3 were 69%, 43%, and 33%, respectively.
3. The amount of shallow traps in the oil-impregnated insulation paper reinforced with nano-TiO₂ increased with increasing nano-TiO₂ content. The space charge distribution in oil-impregnated insulation paper was changed, the maximum electric field distortions decreased, and the value of maximum electric field decreased.

ACKNOWLEDGMENTS

The authors would like to acknowledge support from National Natural Science Foundation of China (51277187) and The National Basic Research Program of China 973 Program; (2009CB724505-1).

REFERENCES CITED

- Abd El-kader, F. H., Gaafer, S. A., Mahmoud, K. H., Mohamed, S. I., and Abd El-kader, M. F. H. (2009). "Electrical conduction in (polyvinyl alcohol/glycogen) blend films," *Polym. Composite* 30(2), 214-220.
- Ahmad, M. S., Zihilif, A. M., Martuscelli, E., Ragosta, G., and Scafora, E. (1992). "The electrical conductivity of polypropylene and nickel-coated carbon fiber composite," *Polym. Composite* 13(1), 53-57.
- Boggs, S. (2004). "A rational consideration of space charge," *IEEE Electr. Insul. Mag.* 20(4), 22-27.
- Chen, G., Tanaka, Y., Takada, T., and Zhong, L. (2004). "Effect of polyethylene interface on space charge formation," *IEEE Trans. Dielectr. Electr. Insul.* 11(1), 113-121.
- Ciobanu, R., Schreiner, C., Pfeiffer, W., and Baraboi, B. (2002). "Space charge evolution in oil-paper insulation for DC cables application," in: *Dielectric Liquids*, ICDL 2002, Proceedings of 2002 IEEE 14th International Conference on (pp. 321-324). IEEE.
- Du, Y., Lv, Y., Li, C., Chen, M., Zhong, Y., Zhou, J., and Zhou, Y. (2012). "Effect of semiconductive nanoparticles on insulating performances of transformer oil dielectrics and electrical insulation," *IEEE Trans. Dielectr. Electr. Insul.* 19(3), 770-776.
- Fleming, R. J., Pawlowski, T., Ammala, A., Casey, P. S., and Lawrence, K. A. (2005). "Electrical conductivity and space charge in LDPE containing TiO₂ nanoparticles," *IEEE Trans. Dielectr. Electr. Insul.* 12(4), 745-753.
- Fothergill, J. C., Dissado, L. A., Alison, J., and See, A. (2000). "Advanced pulsed electro-acoustic system for space charge measurement," in: *Dielectric Materials, Measurements and Applications*, 2000. Eighth International Conference on (IEE Conf. Publ. No. 473) (pp. 352-356). IET.
- Hanley, T. L., Burford, R. P., Fleming, R. J., and Barber, K. W. (2003). "A general review of polymeric insulation for use in HVDC cables," *IEEE Electr. Insul. Mag.* 19(1), 13-24.
- Huang, X., Jiang, P., and Yin, Y. (2009). "Nanoparticle surface modification induced space charge suppression in linear low density polyethylene," *Appl. Phys. Lett.* 95(24), 242905.
- Liu, Z., Liu, R., Wang, H., and Liu, W. (1989). "Space charges and initiation of electrical trees," *IEEE Trans. Dielectr. Electr. Insul.* 24(1), 83-89.
- Liu, R., Jaksts, A., Tornkvist, C., and Bergkvist, M. (1998, June). "Moisture and space charge in oil-impregnated pressboard under HVDC," In: *Conduction and Breakdown in Solid Dielectrics*, 1998. ICSD'98. Proceedings of the 1998 IEEE 6th International Conference on (pp. 17-22). IEEE.
- Liu, R., Takada, T., and Takasu, N. (1993). "Pulsed electro-acoustic method for measurement of space charge distribution in power cables under both DC and AC electric fields," *J. Phys. D. Appl. Phys.* 26(6), 986.
- Mazzanti, G., Montanari, G. C., and Alison, J. M. (2003). "A space-charge based method for the estimation of apparent mobility and trap depth as markers for insulation degradation-theoretical basis and experimental validation," *IEEE Trans. Dielectr. Electr. Insul.* 10(2), 187-197.

- Morshuis, P., and Jeroense, M. (1997). "Space charge measurements on impregnated paper: a review of the PEA method and a discussion of results," *IEEE Electr. Insul. Mag.* 13(3), 26-35.
- Tang, C., Chen, G., Fu, M., and Liao, R. J. (2010). "Space charge behavior in multi-layer oil-paper insulation under different DC voltages and temperatures," *IEEE Trans. Dielectr. Electr. Insul.* 17(3), 775-784.
- Thelakkadan, A. S., Coletti, G., Guastavino, F., and Fina, A. (2011). "Effect of the nature of clay on the thermo-mechanodynamical and electrical properties of epoxy/clay nanocomposites," *Polym. Composite.* 32(10), 1499-1504.
- Tian, F., Lei, Q., Wang, X., and Wang, Y. (2011). "Effect of deep trapping states on space charge suppression in polyethylene/ZnO nanocomposite," *Appl. Phys Lett.* 99(14), 142903-142903-3.
- Tomer, V., Randall, C. A., Polizos, G., Kostelnick, J., and Manias, E. (2008). "High-and low-field dielectric characteristics of dielectrophoretically aligned ceramic/ polymer nanocomposites," *J. Appl. Phys.* 103(3), 034115-034115.
- Wang, Y. Q., Yi, Y., Li, X. G., and Chuan, C. (2009). "Study of the space charge behaviour in polyethylene doped with nano-MgO," *Electric Wire & Cable*, 3, 20-23.
- Zha, J. W., Dang, Z. M., Song, H. T., Yin, Y., and Chen, G. (2010). "Dielectric properties and effect of electrical aging on space charge accumulation in polyimide TiO₂ nanocomposite films," *J. Appl. Phys.* 108(9), 094113-094113.
- Zhang, Y., Lewiner, J., Alquie, C., and Hampton, N. (1996). "Evidence of strong correlation between space-charge buildup and breakdown in cable insulation. Dielectrics and Electrical Insulation," *IEEE Trans. Dielectr. Electr. Insul.* 3(6), 778-783.
- Zhou, Y., Wang, Y., Li, G., Wang, N., Liu, Y., Li, B., and Cheng, H. (2009). "Space charge phenomena in oil-paper insulation materials under high voltage direct current," *J. Electrostat.* 67(2), 417-421.

Article submitted: June 19, 2013; Peer review completed: August 31, 2013; Revised version accepted: September 16, 2013; Published: September 23, 2013.